

Combination of Different Thermal Analysis Methods Coupled to Mass Spectrometry for the Analysis of Asphaltenes and Their Parent Crude Oils: Comprehensive Characterization of the Molecular Pyrolysis Pattern

Christopher P. Rüger,^{*,†,‡,§} Christoph Grimmer,[†] Martin Sklorz,[†] Anika Neumann,[†] Thorsten Streibel,^{†,‡} and Ralf Zimmermann^{†,‡,§}

[†]Joint Mass Spectrometry Centre/Chair of Analytical Chemistry, University of Rostock, 18051 Rostock, Germany

[‡]Joint Mass Spectrometry Centre/Cooperation Group Comprehensive Molecular Analytics, Helmholtz Zentrum München, 85764 Neuherberg, Germany

[§]Aerosols and Health, Helmholtz Virtual Institute of Complex Molecular Systems in Environmental Health (HICE), 85764 Neuherberg, Germany

Supporting Information

ABSTRACT: In this study, the asphaltene and corresponding crude oil, distributed within the Asphaltene Characterization Interlaboratory Study for PetroPhase 2017, were characterized on the molecular level. For this purpose, three different thermal analysis mass spectrometry hyphenations with five diverse ionization techniques varying in selectivity were deployed: (1) thermal desorption/pyrolysis gas chromatography electron ionization (TD/Pyr–GC–EI–QMS), (2/3) thermogravimetry single-photon/resonance-enhanced multiphoton ionization time-of-flight (TG SPI/REMPI TOF–MS), and (4/5) thermogravimetry atmospheric pressure photo-/chemical ionization ultrahigh-resolution mass spectrometry (TG APPI/APCI FT-ICR MS). For the investigated C₇ asphaltene, no mass loss was detected at <300 °C and the pyrolysis phase was dominant, whereas the parent crude oil exhibits a high abundant desorption phase. At roughly 330 °C, pyrolysis begins and mass loss as well as complex mass spectrometric patterns were recorded. The resulting information on the effluent gained by the different soft ionization mass spectrometric approaches was combined with the GC–EI–MS data for structural cross-evaluation. We showed that the combination of the applied techniques leads to a more comprehensive chemical characterization. For the asphaltene, TG SPI TOF–MS shows high abundances of alkanes, alkenes, and hydrogen sulfide during pyrolysis. TG REMPI TOF–MS is selective toward aromatics and reveals clear patterns of polyaromatic hydrocarbons (PAHs) and minor amounts of nitrogen-containing aromatics tentatively identified as acridine- or carbazol-like structures. GC–EI–MS provides information on the average chain length of alkanes, alkenes, and PA(S)H. Both atmospheric pressure ionization techniques (APPI and APCI) hyphenated to FT–MS showed CHS (in particular, benzothiophenes) and CH as dominant compound classes, with an average number of condensed aromatic rings of 2–4. Combining the information of all techniques, including the average asphaltene mass obtained by field desorption experiments and aromatic core size received by collision-induced dissociation, the archipelago-type molecular structure seems to be dominant for the investigated asphaltene.

INTRODUCTION

The chemical composition of petroleum and petrochemical products is crucial for their processing and economic utilization.^{1–3} Even with state-of-the-art analytical instrumentation, the analysis of heavy petroleum and its fractions as well as from unconventional petroleum sources, such as oil sands, is still a challenge.^{4,5} Especially, for the asphaltene fraction, a part of the petroleum that is soluble in toluene and insoluble in a small paraffin, such as *n*-heptane, only a few standardized analysis methods exist.⁶ These ultracomplex mixtures with high aromatic content, besides other heavy constituents, cause particular problems for traditional approaches, e.g., chromatographic and high-resolution mass spectrometric techniques. A molecular understanding of the asphaltene fraction is however of particular interest because these species are known to cause flow assurance and processing issues in up- and downstream processes.^{6,7}

State-of-the-art techniques for the chemical characterization of asphaltenes on the molecular level are mainly mass spectrometric approaches, such as direct infusion atmospheric pressure ionization ultrahigh-resolution mass spectrometry.^{4,8,9} In addition, high-field nuclear magnetic resonance (NMR) spectroscopy and absorption spectroscopic approaches, such as X-ray absorption near edge structure (XANES)^{10–12} as well as high-performance liquid chromatography, are deployed.¹³ Thermal analysis (TA), regarding evolved gas analysis, coupled to various analytical detectors has also become a powerful tool in petroleum analysis and other areas.^{14–19}

Special Issue: 18th International Conference on Petroleum Phase Behavior and Fouling

Received: September 15, 2017

Revised: November 30, 2017

Published: December 4, 2017

Besides spectroscopic approaches, such as infrared spectroscopy for fingerprint pattern or small-molecule quantification,^{15,20,21} mass spectrometry is the favored coupling technique.^{14,16,18} For heavy petroleum, thermal analysis is primarily applied for studying the evaporation pattern as well as the thermal decomposition products at an elevated temperature during pyrolysis.^{22–24} Pyrolysis gas chromatography was conducted extensively with low resolving mass analyzers and hard ionization to study thermal decomposition products since the 1980s.^{25–31}

Unfortunately, until now, no single mass spectrometric technique is capable of a comprehensive analysis of the complex pyrolysis effluent. Therefore, choosing an ionization source is crucial, and different methods will cover different chemical spaces.³² For the thermal analysis of petroleum fractions, most often nominal resolving mass analyzers with hard ionization are used, which enable robust pattern information.^{15,33} Nonetheless, soft ionization techniques become more important in mass spectrometry and thermal analysis coupling. The generation of molecular ions, instead of an intense fragment pattern, reduces the complexity of the mass spectra and allows for an easier molecular assignment. In previous studies, we applied various soft ionization techniques for thermal analysis, such as photoionization^{23,34–37} and chemical ionization.^{38–41} With the selection of a particular soft ionization technique, control of selectivity can be achieved. In the case of resonance-enhanced multiphoton ionization (REMPI), aromatic compounds are selectively ionized,^{42,43} whereas atmospheric pressure photoionization (APPI) reveals a high ionization efficiency for aromatic and sulfur-containing species and atmospheric pressure chemical ionization (APCI) reveals a high ionization efficiency for medium-polar and polar constituents.^{32,44–47} We applied TA with soft ionization mass spectrometric detection for a wide range of applications, e.g., nut and coffee roasting,^{36,48,49} crude oils,^{23,24,37} biomass/tobacco pyrolysis,^{34,35,41} elemental sulfur evaporation,⁵⁰ polymers,³⁷ and dissolved organic matter.⁵¹ Asphaltene pyrolysis has not been studied before with photoionization (PI) techniques, with either vacuum PI or atmospheric pressure PI.

All ionization techniques cover a particular molecular space and exhibit a certain part of the chemical signature of a complex mixture. In this study, the results of three different thermal analysis approaches equipped with five different ionization techniques are combined for a more comprehensive analysis of the effluent of an asphaltene and its parent crude oil. For this purpose, the heptane (C_7) asphaltene and parent crude oil of the Asphaltene Characterization Interlaboratory Study for PetroPhase 2017 were investigated. Asphaltenes are one of the most complex natural mixtures with a variety of hetero-elements and chemical functionalities, spanning a broad mass range. Over the last few decades, a lot of effort has gone into deciphering their molecular architecture, whereby two opposed models are discussed: island (large aromatic core with side chains) and archipelago (linker connected smaller aromatic cores). As shown for pyrolysis gas chromatography in the literature, the thermal decomposition products of the macromolecular structure should give information about the respective building blocks and add valuable information to the molecular architecture debate.

Five different ionization schemes were applied with electron ionization (EI) as a hard and universal technique, single-photon ionization (SPI) as a soft and universal method, REMPI as an aromatic-selective and soft technique, as well as atmospheric pressure chemical and photoionization (APCI/APPI). This study

aims to show the advantages and limitations of the individual methods and the potential of combining their results. High-resolution mass spectrometry will give information about the elemental composition, whereas pyrolysis gas chromatography will add structural aspects and SPI will provide information on the thermally cracked side chains. We hypothesize that thermal analysis mass spectrometry can contribute significantly to unravel asphaltene composition and structure when several techniques are combined, with the interlaboratory asphaltene study as an ideal case study as a result of the extensive research conducted on the same asphaltene sample.

MATERIALS AND METHODS

Material. In this study, a heptane (C_7) asphaltene and the corresponding parent crude oil (a Colombian heavy crude oil, with an American Petroleum Institute (API) gravity of 12°)⁵² were investigated. The samples were received within the Asphaltene Characterization Interlaboratory Study for PetroPhase 2017 and had been prepared by the group of Marianny Y. Comariza at the Industrial University of Santander (Colombia).⁵² In brief, asphaltenes are precipitated using the ASTM D6560-12 procedure with *n*-heptane under sonication (110 W and 40 kHz), which decreased co-precipitants significantly. Four Soxhlet extraction steps were deployed as an additional cleaning procedure for an efficient removal of occluded compounds of the maltene fraction to receive the final cleaned asphaltene sample. Additional information on the elemental composition is given in Table S1 of the Supporting Information.

Instrumentation. Three thermal analysis setups coupled to different mass spectrometric systems were deployed within this study: (1) thermal desorption/pyrolysis gas chromatography with electron ionization and quadrupole mass spectrometric detection (TD/Pyr-GC-EI-QMS); (2/3) thermogravimetry photoionization [single-photon ionization (SPI) and resonance-enhanced multiphoton ionization (REMPI)] with time-of-flight mass spectrometric detection (TG SPI/REMPI TOF-MS), and (4/5) thermogravimetry atmospheric pressure photo- and atmospheric pressure chemical ionization ultrahigh-resolution mass spectrometry (TG APPI/APCI FT-ICR MS). The schematic setup of the three mass spectrometric hyphenations and their corresponding ionization techniques is given in Figure 1. Additionally, the figure depicts survey diagrams of the associated asphaltene measurements.

For the (1) thermal desorption/pyrolysis gas chromatographic analysis, 10 μ L of the diluted parent crude oil (1:100 in dichloromethane) and roughly 0.5–0.9 mg of the solid asphaltene were injected into the pyrolyzer (model PY-2020iD, double-shot pyrolyzer, Frontier Laboratories) mounted onto a HP 6890 gas chromatograph.^{53,54} The sample material undergoes two steps: (1) a thermal desorption process at 300 $^\circ$ C and (2) a pyrolysis step at 500 $^\circ$ C, each held for 1 min. To separate the evolved gas mixture, a 30 m SGE-BPX5 column (250 μ m inner diameter, 0.25 μ m film, helium at 99.999%, and head pressure at 0.4 bar) was used with the following temperature program: hold for 10 min at 50 $^\circ$ C, ramp to 330 $^\circ$ C with 10 K/min, and hold for 20 min. The effluent from the column was ionized by a 70 eV electron ionization source and analyzed by a quadrupole mass spectrometer. Mass spectra were recorded in scan mode from m/z 10 to 500. Data were analyzed by AMDIS version 2.62 and Bruker DataAnalysis 4.0 SP 1. In brief, Bruker DataAnalysis was used for fast assessment of the data and obtaining a qualitative overview, e.g., survey view, extracted ion chromatograms, and averaging of time segments. Afterward, AMDIS was used for finding chromatographic features (deconvolution) and validation of fragment spectra with the National Institute of Standards and Technology (NIST) database (NIST MS Search 2.0).

For setup 2/3, the volatile and semi-volatile constituents of the effluent from a thermal balance were analyzed by single- and resonance-enhanced multiphoton ionization (SPI/REMPI). For this purpose, a thermobalance (STA 409, Netzsch Gerätebau, Selb, Germany) was directly hyphenated to the ionization source of the mass spectrometer

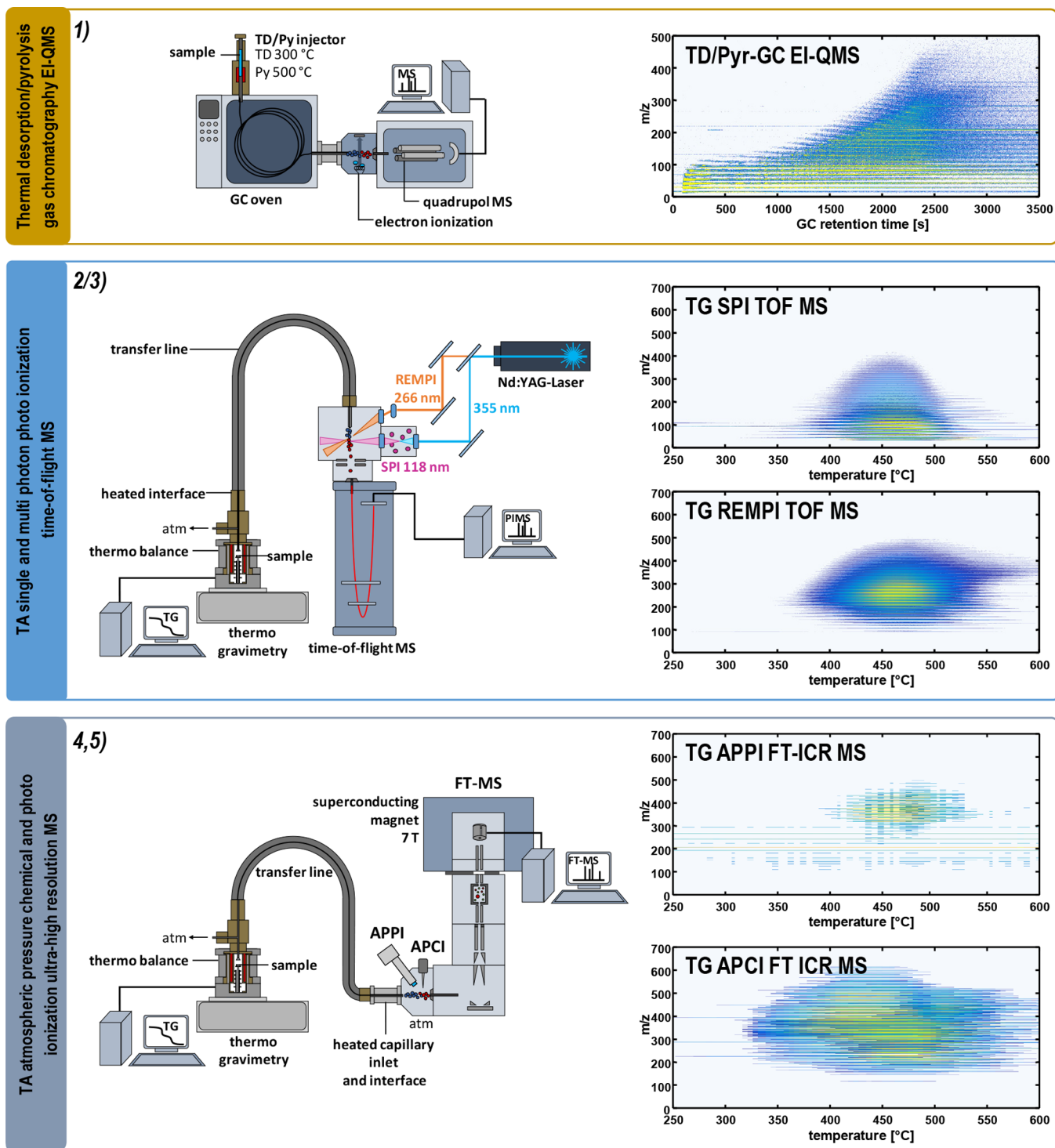


Figure 1. Schematic overview of the deployed thermal analysis mass spectrometry hyphenations: (1) thermal desorption/pyrolysis gas chromatography with electron ionization quadrupole mass spectrometric detection (TD/Py-GC-EI-QMS); (2/3) thermogravimetry photoionization with time-of-flight mass spectrometric detection (TG SPI/REMPI TOF-MS), and (4/5) thermogravimetry atmospheric pressure photo-/chemical ionization ultrahigh-resolution mass spectrometry (TG APPI/APCI FT-ICR MS). Survey views (retention time/temperature versus m/z) are given on the right-hand side for each applied technique on the analysis of the Asphaltene Characterization Interlaboratory Study for PetroPhase 2017 asphaltene sample.

via a heated interface and transfer line (1 2.25 m, 280 μm inner diameter, and 280 °C).^{55,56} A few milligrams of the sample material were placed on an aluminum oxide crucible without any sample pretreatment. Thermal analysis was carried out with a heating rate of 10 K/min under a nitrogen atmosphere (60 mL/min) from 30 to 800 °C. At 800 °C, nitrogen is partially replaced by air (40 mL/min synthetic air

and 20 mL/min nitrogen), yielding an oxidative atmosphere. Evolved gas was sampled as a result of the pressure difference between the balance at atmospheric pressure and the ion source at vacuum (roughly 3×10^{-4} mbar). The subsequent SPI and REMPI TOF-MS analysis is described in detail elsewhere.^{23,34,57} In brief, for SPI, 355 nm laser pulses (25 mJ pulse energy, 10 Hz repetition rate, and 5 ns

pulse width), generated from a Nd:YAG laser (Surelite III, Continuum, Inc., Santa Clara, CA, U.S.A.), were sent through a xenon-filled gas cell (Xe 4.0, 12 mbar), yielding vacuum ultraviolet photons (118 nm and 10.5 eV). For REMPI, the Nd:YAG fundamental wavelength is frequency-quadrupled (4.7 eV and 266 nm). The molecular ions formed by either REMPI or SPI are recorded from m/z 5 to 500 with TOF-MS using a multichannel plate detector. Data processing and analysis were carried out with the instrument-specific LabView graphical user interface and self-written MATLAB scripts.

The third mass spectrometric setup (4/5) is composed of a thermobalance (TG 209, Netzsch Gerätebau, Selb, Germany) coupled to a modified Bruker GC-APCI II source, which allows us to carry out APCI with a stainless-steel corona needle (3 μ A corona current) as well as APPI with a Kr vacuum ultraviolet (VUV) lamp (10/10.6 eV and 124/117 nm).⁵⁸ The temperature program of the thermobalance with a constant flow of 200 mL/min nitrogen was 2 min isothermal at 20 °C, ramp to 600 °C with 10 K/min, and hold for 10 min at 600 °C. The evolved mixture was sampled via a 300 °C interface and 280 °C transfer line into the ion source. In contrast to setup 2/3, the gas sampling was achieved by a slight overpressure of 8–10 mbar in the thermobalance compared to the atmospheric pressure in the ionization source. For mass spectrometric detection, a Bruker Apex II ultra FT-MS equipped with a 7 T superconducting magnet was used. Mass spectra were recorded from m/z 100 to 2000 with a four megaword transient, resulting in a resolving power of roughly 300 000 at m/z 400. A broad band spectrum with five microscans was recorded, alternating with a collision-induced dissociation (CID) spectrum of the whole mass range at 30 V with five microscans, resulting in an overall

acquisition rate of 0.2 Hz. A detailed description of the APCI setup can be found elsewhere.⁴¹ Atmospheric pressure chemical and photo-ionization were deployed in positive ion mode. For APCI, roughly 1–2 mg of the parent crude oil and asphaltene were analyzed, whereas for APPI, 3–5 mg of the sample was placed into the aluminum crucible. Please note that the source was optimized for gas chromatography APCI, leading to a lower sensitivity in APPI mode.

RESULTS AND DISCUSSION

All of the applied techniques exhibit certain characteristics, such as high mass resolving power and accuracy for the hyphenation of thermogravimetry to atmospheric pressure ionization FT-MS, vacuum ionization avoiding matrix effects, or additional gas chromatographic information from the two-step desorption/pyrolysis system. This diversity results in five complex and diverse data sets (see Figure 1), and their information has to be efficiently combined to allow for a comprehensive description of the effluent. In Figure 2, a simplified schematic of one possible data analysis route is given as a roadmap for the analysis throughout this study.

One advantage of the thermogravimetric assemblies (2/3 and 4/5) is the recording of the temperature-dependent mass loss curve, which reveals quantitative information on the volatility and decomposition, which is not accessible with the TD/Py-GC setup. The mass loss curves showed no significant desorption step and a relatively sharp pyrolysis signal peaking at 435–460 °C with

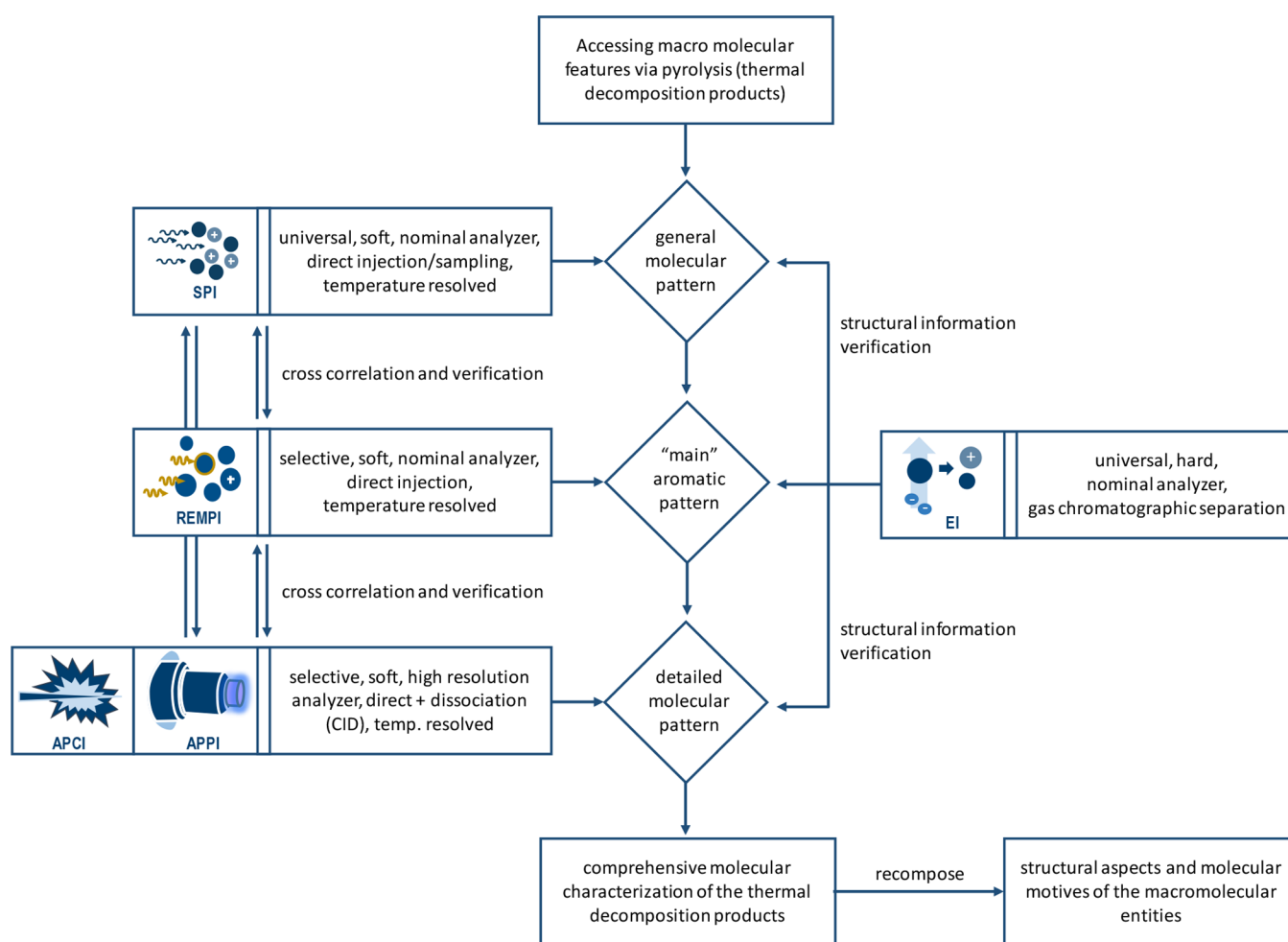


Figure 2. Flowchart for the evaluation of the applied thermal analysis mass spectrometric data sets. The data from techniques not involving chromatographic separation are backed up partially with information from GC and among themselves.

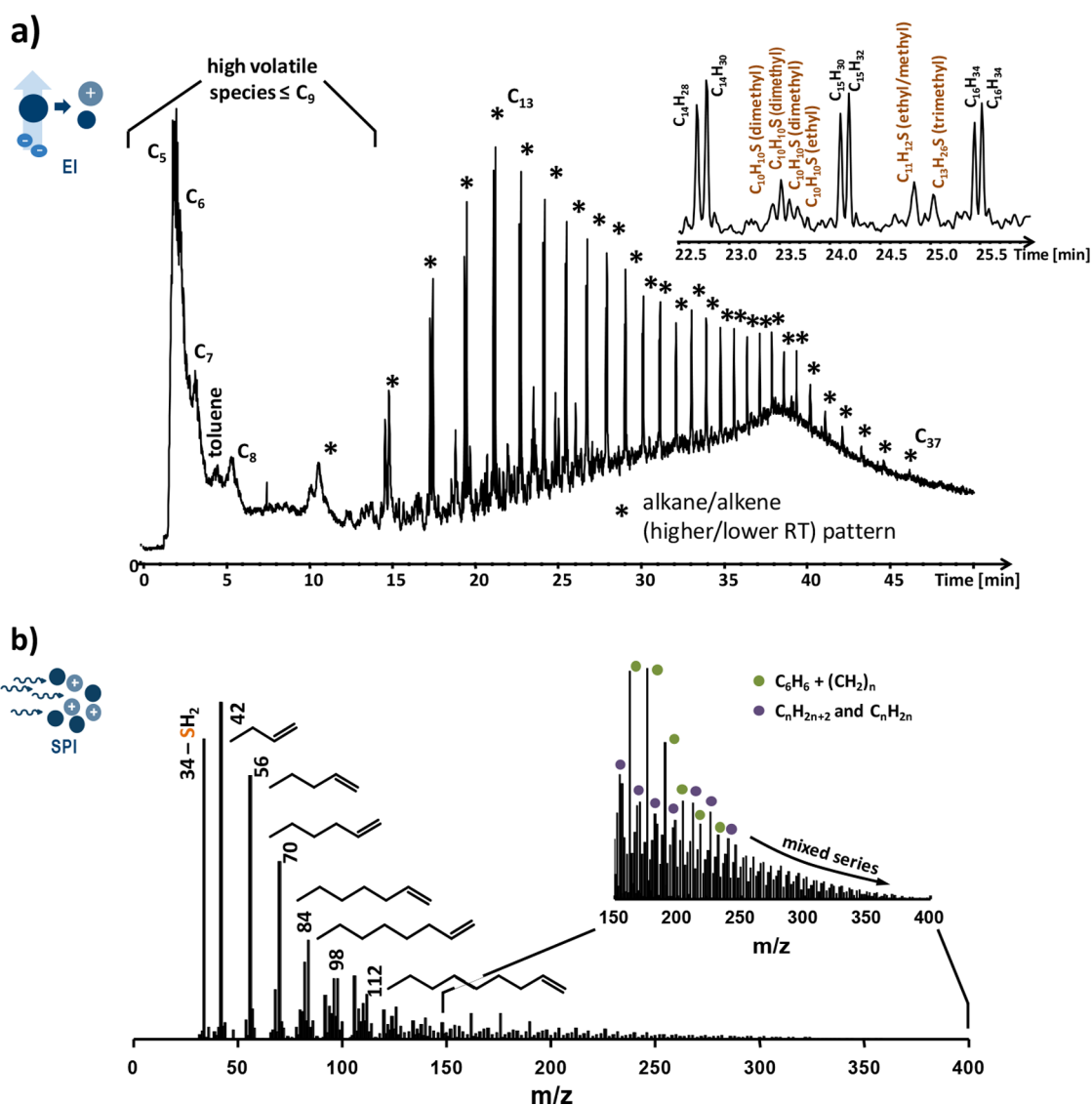


Figure 3. (a) Total ion count gas chromatogram for the 500 °C pyrolysis EI-QMS measurement of the asphaltene. Low mass hydrocarbons down to C_2 were detected, but chromatographic separation was insufficient. Starting with C_{10} , a defined alkane and alkene pattern is observed, whereas the enlarged section reveals alkylated benzothiophene isomers. (b) Averaged SPI mass spectrum for the asphaltene pyrolysis with a high abundance alkene pattern. Within the expanded part of the SPI mass spectrum, a continuing benzene, alkane, and alkene pattern can be observed.

a mass loss of 47–49 wt % (Figure S1 of the Supporting Information). The thermal behavior is in good agreement with the chemical evolved gas analysis data from TD/Pyr-GC as well as with the mass spectrometric response of the TG-coupled spectrometer. In contrast, the parent crude oil exhibits an intense desorption phase with a mass loss of roughly 60 wt % before 300 °C and a further mass loss of approximately 30 wt % in the pyrolysis phase (300–600 °C). An amount of approximately 49 wt % for the asphaltene and 5 wt % for the parent crude oil remained as a deposit and is rapidly decomposed under an oxidative atmosphere at 800 °C. This deposit can be assigned to carbonized species formed during pyrolysis, e.g., graphite. Literature shows that the yield of volatile matter in the pyrolysis phase correlates with the aliphatic content in petrochemicals, and therefore, a high proportion of the mass loss will be caused by dealkylation of aromatic species.⁵⁹ In summary, the hypothesis that the interlaboratory asphaltene sample does not contain significant amounts of volatile

or semi-volatile species can be stated and is in agreement with the literature for other asphaltenes.⁶⁰

Pyrolysis Gas Chromatography. The pyrograms obtained by pyrolysis gas chromatography at 500 °C were analyzed as shown in the literature to obtain the average side-chain length, sulfur compounds versus aliphatic compounds, and to indicate the presence of SO_2 as well as CO_2 .^{28,61} The low ionization efficiency dependence of the EI concerning the molecular structure and size is a useful advantage compared to chemical and photoionization. Primary pyrolysis signals were aliphatic side chains up to a length of 37 carbons (C_{37}). SO_2 (m/z 64) was found to a very low extent compared to H_2S (m/z 34). This finding indicates nearly oxygen-free conditions. Thiophenic species were found to be more abundant than H_2S , indicating thiophene sulfur constituents dominant compared to thiols. The comparison between sulfur compounds and aliphatic species revealed a strong dominance of aliphatic species, with 2 orders of magnitude higher abundance. The average aliphatic side-chain length turned out to be 8.2 ($m/z \sim 120$), identified by

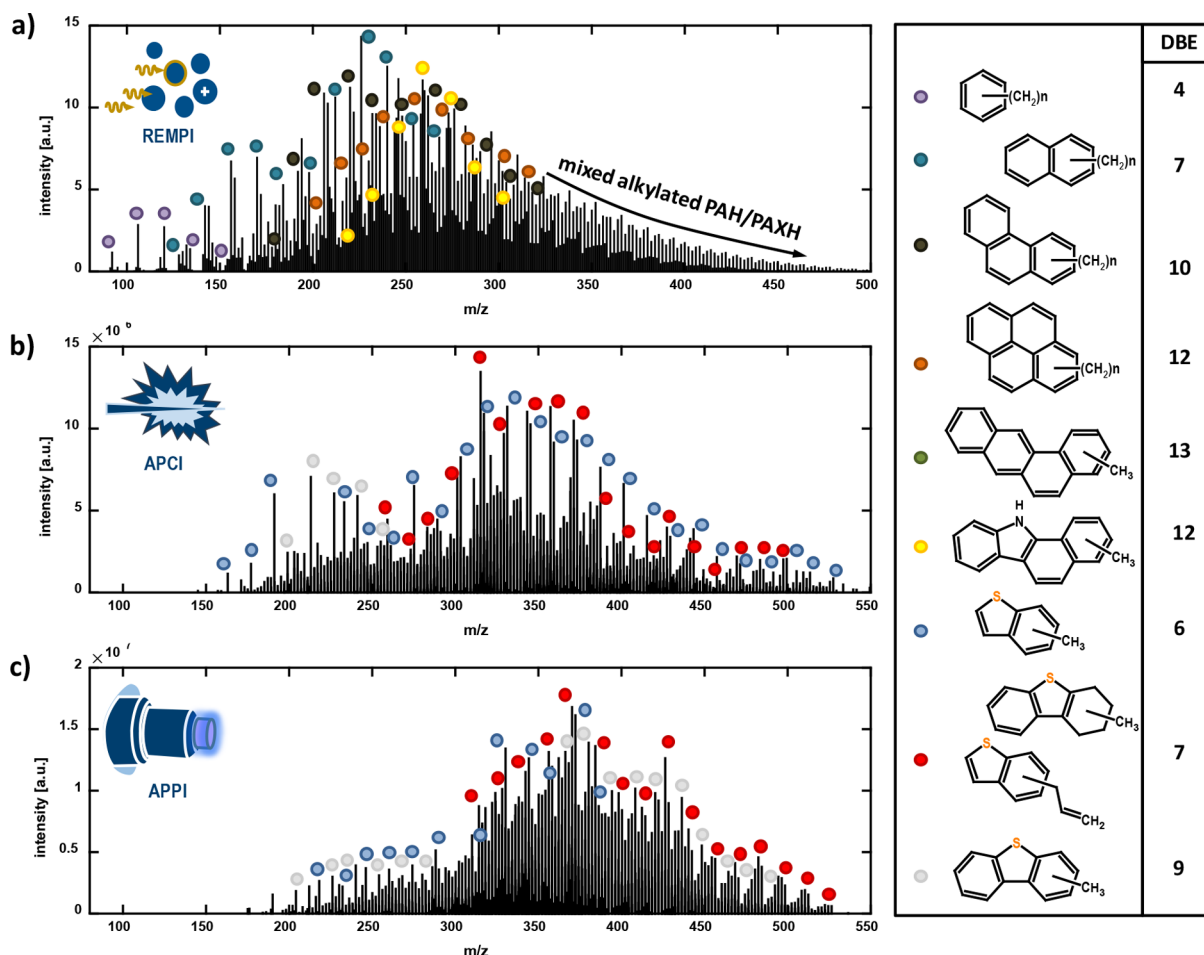


Figure 4. Average mass spectra of the asphaltene pyrolysis for (a) REMPI TOF-MS, (b) APCI, and (c) APPI FT-ICR MS. Tentative assignments of selected aromatic alkylated series as well as their structure and DBE are given on the right side. PAXH = heteroatom (X = N, S, and O)-containing polycyclic aromatic hydrocarbons (PAHs).

the alkane and alkene main fragments m/z 55 and 57, which is slightly higher than values from the literature (Figures S2–S5 of the Supporting Information).^{28,61} Branched alkane/alkene species were only present in minor abundance in the effluent compared to the *n*-isomeric species. Nonetheless, for larger carbon numbers, the separation power is insufficient for a complete separation and no clear isomeric information can be given on species larger than C₁₈. They may have a higher proportion of branched isomers as the ratio of branched/linear species increases with increasing m/z . The investigation of the aromatics on the basis of m/z 91 for the alkyl benzene species and m/z 162 and 176 for benzo- and dibenzothiophenes revealed an intricate pattern of sulfur species, captured in more detail with APPI and APCI. Furthermore, the thiophene species with the lowest molecular weight were found to be 2-ring benzothiophenes, whereas for hydrocarbons, alkylated benzene species (1 ring) were found. These 1-ring aromatics can be eventually formed during pyrolysis from naphthenic derivatives and, moreover, might be overrepresented as a result of their GC optimal volatility range. The fragmentation of the EI hinders the detection of the molecular ion and, in addition to that, a more detailed assignment, e.g., of naphthenic constituents.

Single-Photon Ionization. For the single-photon ionization, a universal and soft ionization technique,^{43,62} typical petroleum patterns with homologue series of m/z 14 (CH₂) and m/z 2 (H₂) spacing were observed for the parent crude oil

as well as asphaltene. The spectra (Figure S6 of the Supporting Information and Figure 3b) covered a mass range from m/z 34 to approximately 450. The higher contribution of intact desorbed species in the total average parent crude oil spectra (89% TIC < 350 °C) leads to a higher intensity-weighted molecular weight (m/z 147.9), whereas the asphaltene spectrum is dominated by thermally induced dealkylation products (average m/z 100.8, 97.3% TIC > 350 °C) partially identified by pyrolysis GC. The asphaltene pattern peaks at m/z 42 (C₃-alkene and propene), with m/z 34 (H₂S) the second dominant, whereas the crude oil pattern peaks at m/z 120 (C₃-alkylated benzene) with m/z 156 (C₃-alkylated benzene) as the second dominant. Comparing only the pyrolysis pattern of the parent crude oil and the asphaltene, SPI shows a high similarity. In more detail, the abundance of the alkene pattern in the asphaltene spectra exponentially decreases for heavier alkenes. This finding is in good agreement with the pyrolysis GC, for which the C₅ alkene was found to be the most abundant alkene (because C₄ was too volatile for detection). Assuming an alkylated homologous series starting at m/z 42 (m/z 42 + $n \times 14$) for the alkenes and isobaric cycloalkanes, an average alkene length of C_{9,1} can be calculated for the asphaltene. Isobaric species for this series can be alkylated cycloalkanes with 1 saturated ring, which were found only in minor abundance in the GC pyrograms and are less common as stable products in pyrolysis.^{59,63} The average alkene length

estimated with the universal soft SPI is congruent to the pyrolysis GC data obtained with the universal hard electron ionization, although the photoionization cross section has to be taken into account. Fortunately, in SPI, the cross sections range only between a factor of 2 and 3 within one compound class.⁵⁴ The substantial occurrence of H₂S is caused by the decomposition of organic sulfur constituents, mainly thiols. On the basis of this signal, the sulfur content of the asphaltene is far higher compared to the parent crude oil, which was also found in the respective GC data. Pyrolysis GC–EI–QMS was optimized for larger constituents; hence, species below C₉ do not reveal a good peak shape (Figure 3). Nonetheless, the main effluent components can be verified by the electron ionization fragment spectrum as starting from the C₅ alkane/alkene at a retention time of roughly 2 min. As of a retention time of 15 min, the gas chromatogram exhibits a clear pattern for alkanes and alkenes, peaking at C₁₃. Pyrolysis of the macromolecular asphaltene structures results to a large extent in the release of smaller alkyl chains below C₇ by cracking as well as notable amounts of larger alkenes above C₁₀. Nonetheless, also very long alkyl chains, which can either originate from a linker or more likely from a core structure alkylation side, can be found (up to C₃₇, $m/z \sim 520$). The cracking process during pyrolysis is a complex mixture of reactions economically used by refineries (thermal cracking/visbreaking, 450–750 °C, usually at high pressures around 70 bar). Carbon–carbon single bonds are broken, and free radicals are formed. A series of reactions then lead to a high proportion of terminal alkenes. We can assume that long side chains more readily undergo cracking than sterically hindered linker sites. Besides the dominant alkene pattern, a less abundant distribution pattern of thermal decomposition products with higher m/z can be seen in the survey view of SPI TOF–MS (Figure 1). These patterns can be partially attributed to aromatic species, which were already briefly discussed in the pyrolysis GC data. A more specific approach, such as REMPI, which is highly selective for aromatic constituents, can be beneficial, particularly because the m/z values of alkane and alkene/cycloalkane species coincide with aromatic alkylation series. Alkenes formed by cracking are highly abundant. Thus, as a result of dynamic range aspects, a more selective technique is advantageous too.

Resonance-Enhanced Multiphoton Ionization. Figure 4 provides a more selective view on the complex asphaltene pyrolysis mixture. The two-photon process in REMPI ionizes species with an ionization energy (IE) below 9.32 eV (2×4.66 eV) and a stable intermediate state. Consequently, solely aromatics can be found. A pattern with the same characteristic CH₂ group spacing as with SPI can be observed. The spectrum peaks at m/z 226, most likely C₇-alkylated naphthalenes. The 2–4-ring polycyclic aromatic hydrocarbons dominate the spectrum. At higher masses, the series overlap and no clear assignments are possible. It must be kept in mind that REMPI ionization efficiencies span orders of magnitude;^{65,66} in comparison to, e.g., naphthalene, sulfur-containing benzothiophenes are ionized with a 100-fold lower efficiency, whereas alkanes overlapping the aromatic alkylation series are not ionized at all. Nitrogen-containing species will be found on odd m/z values (nitrogen rule), and carbazole and acridine homologue alkylation rows were tentatively identified. With the relative measured abundances, an aromatic ring size of 3–4 with a main alkylation length of C_{3–10} can be revealed for the asphaltene. The average alkylation length of the individual ring sizes was found to be 2–3 for benzene, 8–9 for naphthalene, and slightly

lower for condensed aromatics, with 3–5 rings (6–8). The relatively low average alkylation length results from the cracking process during the pyrolysis.

Atmospheric Pressure Ionization. For REMPI, assignments of probable chemical structures rely on literature knowledge and the ionizable chemical space, e.g., selectivity to aromatics and cross sections. Ultrahigh mass resolution and mass accuracy, as routinely delivered by FT–MS instruments, allow for a mathematical calculation of the elemental composition. Assignment to the summed APPI and APCI FT–ICR MS spectra revealed roughly 800 and 1250 distinct chemical formulas. Grouped into compound classes, it was found for both techniques that CHS species are most dominant (APCI, 58% TIC; APPI, 58% TIC), whereas the CH class is the second dominant (APCI, 25% TIC; APPI, 21% TIC), followed by the CHS₂ class (APCI, 10% TIC; APPI, 18% TIC). In APCI, oxygenated species are present with a higher abundance compared to APPI but still only account for approximately 5% TIC (CHSO, 2.5% TIC; CHO, 1.9% TIC). The low abundance of oxygenated species in asphaltene analysis was also reported in the literature.^{45,67} In both spectra, CHS_{0–2}O_{0–3} class species account for more than 97% of the overall intensity. CHN class species were only found with a very low abundance (<1% TIC). This phenomenon can be explained by the high ionization efficiency of CH and CHS class constituents in positive polarity mode. In comparison to the complete temperature range of the parent crude oil, the asphaltene exhibits a higher abundance of sulfur species and a decreased proportion of CH, CHSO, and CHO_{1–2} (Figure S7 of the Supporting Information). Nonetheless, if only the pyrolysis phase of the parent crude oil is taken into account, the data are consistent with the asphaltene compound class pattern.

Aside from that, the elemental composition assignment allows for an assessment of the aromaticity by the double bond equivalent (DBE) value.⁶⁸ For APCI, an intensity-averaged DBE of roughly 7.8 was detected, whereas for APPI, the value is 9.1, corresponding to a 2–3-ring system. Figure 4 visualizes the dominant homologue row of three selected CHS class members. Both API spectra reveal a pattern peaking at m/z 320–360, corresponding to an alkylation grade of 8–14. The average DBE is slightly higher for the CHS₂ class and similar between CHS and CH constituents. The deviation in average DBE between the API techniques is caused by the slightly shifted observed chemical space. Furthermore, the biased molecular weight distribution of FT–MS compared to TOF data has to be mentioned. A longer storage time for the CID experiments revealed the presence of larger aromatic moieties, with an average DBE value of 13 and 11.7 for APCI and APPI, respectively. With CID, the different tentative assignments, i.e., (1) small aromatics with alkene side chains versus (2) larger ring systems with saturated positions, can be proven. If the double bond is located in the side chain (case 1), the DBE 7 homologue row should decrease significantly in the fragmented spectra compared to the DBE 6 or 9 row. This reduction was not observed, leading to the hypothesis that a large proportion is given by partially saturated ring systems (case 2) rather than the particular alkene isomer (case 1). The DBE patterns of asphaltene pyrolysis are similar to those from the pyrolysis phase of the parent crude oil. The similarity between the pyrolysis phases of the asphaltene and the parent crude oil shown by all techniques suggests that asphaltene species cause a high proportion of the pyrolysis of the crude oil. Figure 5 visualizes the revealed chemical space by example of

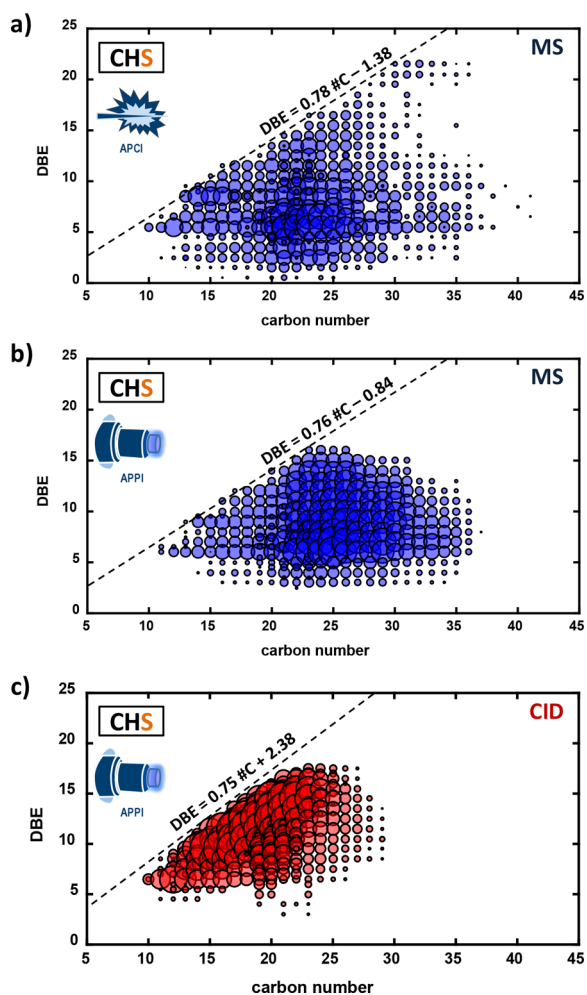


Figure 5. Carbon number versus DBE visualization for the (a) APCI and (b) APPI assignments of the CHS₁ class as well as for the (c) CHS₁ class assignments observed for the asphaltene sample via APPI–CID. Additionally, the results of the planar limit-assisted calculation are given.

the CHS class and carbon number versus DBE diagram. Elemental compositions with a carbon number up to 37 were found ($m/z \sim 520\text{--}550$) spanning a DBE range from 2 to 22 in APCI, whereas APPI reveals a narrower DBE spread from 3 to 16. Interestingly, thermal decomposition products identified with SPI and GC are in the same m/z range. Furthermore, the elemental composition assignments received by the high-resolution FT–MS CID spectra can be used for planar limit-assisted structural interpretation of the aromatic building blocks, which give information on how the rings are arranged.^{69,70} For this purpose, the lower carbon number limit of the distribution is fitted linearly. A slope of 0.78 for APCI and 0.76 for APPI was found, corresponding to a linear benzene ring addition (*cata*-condensed, e.g., anthracene, naphthalene, and biphenylene) with a slight proportion of nonlinear addition (*peri*-condensed, e.g., pyrene, perylene, and coronene). These values are in good agreement with the fittings observed for the CID spectra. The CHS₂ class revealed the highest slope, which indicates condensed aromatic ring systems as a more dominant structural motive.

The carbon number versus DBE diagrams show a horizontal shift for the CID spectra compared to the non-fragmented as a result of (neutral loss) dealkylation with preservation of the

parent aromatic structure. This finding proves that the observed thermal decomposition products have a single aromatic core architecture, which is alkylated by side chains containing no additional ring systems. An average dealkylation, as calculated by the difference of the intensity-weighted average m/z of the parent and CID spectra divided by 14 (m/z of CH₂), of 2.1 for APCI and 6 for APPI was found. A more precise estimation of the average alkylation length can be performed by subtraction of the mean carbon number determined for the non-fragmented spectra and the lowest carbon number found in the CID experiment for each DBE value. This approach results in an average alkylation length of 6–10. The CID voltage was kept rather low to prevent other fragmentation processes. Nonetheless, this precaution will not lead to a complete dealkylation, and alkylated constituents are still observed in the CID pattern. Thus, the real average alkylation length may be somewhat higher. With this in mind and assuming the structures proposed in Figure 4, an average alkylation state of 10–13 is more realistic. The parent crude oil reveals a higher value with the same approach. This finding agrees with the literature that the alkyl chain length decreases in the order of saturates > aromatics > resins > asphaltenes.⁶⁹ Furthermore, it has to be kept in mind that, in this study, thermal decomposition products were investigated and the intact asphaltene molecules might consist of several of the observed aromatic cores and alkyl chains.

Data Combination. In the Asphaltene Characterization Interlaboratory Study for PetroPhase 2017, among many other techniques, field desorption mass spectrometry (FD–MS), a universal and soft ionization approach, was conducted with the same sample (Figure S8 of the Supporting Information). A mean molecular mass (M_w) of m/z 1267 and an intensity-weighted molecular mass (M_n) of m/z 974 with a polydispersity (M_w/M_n) of 1.30 was revealed with this approach. Less stable molecules can undergo a certain degree of dissociation in FD–MS. Therefore, the prediction of the mean intact mass is a rather conservative assumption and might be higher. Nonetheless, field ionization mass spectrometric investigations as well as fluorescence depolarization techniques on asphaltenes obtained an average molecular weight of m/z 700–750,^{71–73} which is in the same order of magnitude, and the dissociation effect might be very small. Dependent upon the type of applied ionization techniques, the following intensity-weighted average mass for the thermal decomposition product were obtained: m/z 100, 270, 366, and 337 for SPI, REMPI, APPI, and APCI. DBE can be calculated from the molecular weight, given by FD–MS, and elemental analysis.⁶⁸ This calculation results in an average DBE value of 31.6 for an average intact molecular weight of m/z 974, a carbon content of 81.5 wt %, a hydrogen content of 7.4 wt %, and a nitrogen content of 1.3 wt %. If we assume an average DBE of 10 (3 condensed aromatic rings) and m/z of 270 (taken from the REMPI TOF data) for the aromatic pyrolysis products, and an average DBE of 1 (taken from SPI TOF, representing mainly non-polyaromatic products), the intact macromolecular asphaltene structure is composed of roughly three aromatic cores (Figure 6 and Figure S9 of the Supporting Information). A remaining mass of approximately m/z 200 (~ 14 CH₂-units) is contributed by additional alkylation sites and linkers. As mentioned above, the intact mass assumption might be higher, consequently contributing to alkylation sites and saturated linker motives. Figure 6 summarizes the findings of the individual soft ionization techniques, indicating their overlap

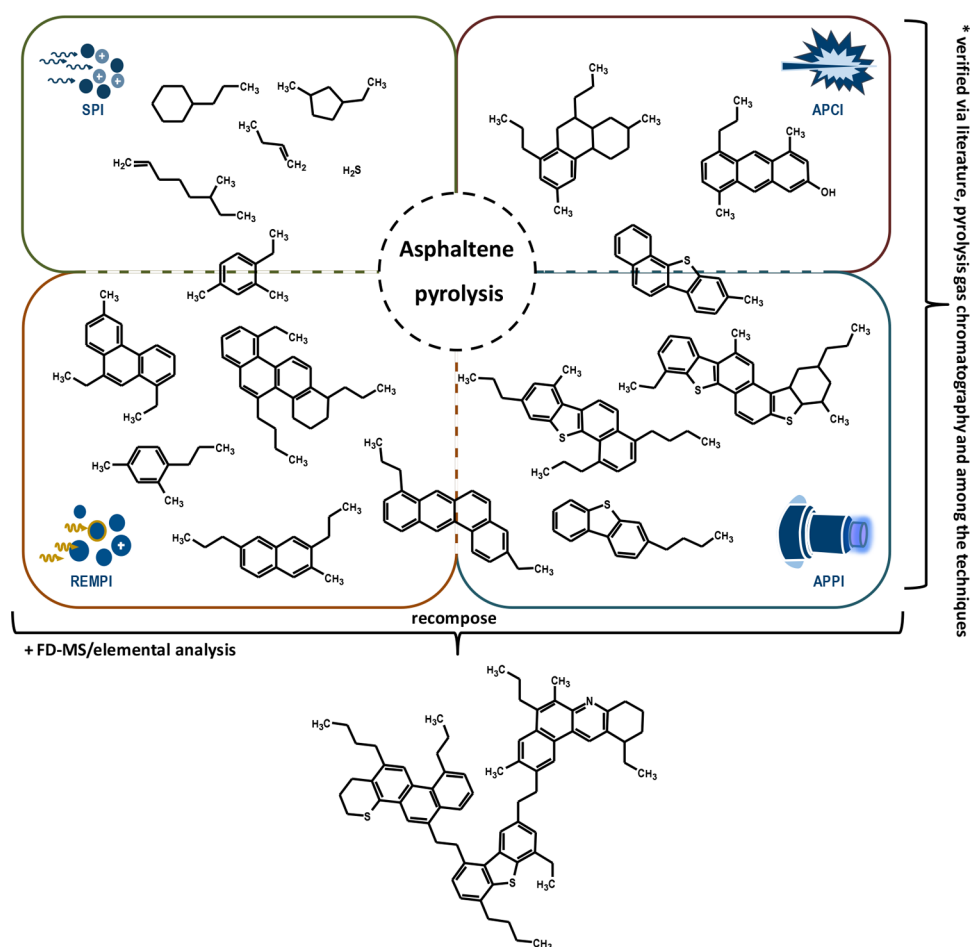


Figure 6. Schematic representation of the most likely tentative assignments and the chemical space, which is covered by the individual techniques as well as their overlap. The molecular structures and moieties can be recomposed to an exemplary asphaltene structure.

as well as giving a tentative asphaltene structure as revealed here by the presented pyrolysis approach and FD–MS.

The chemical nature of asphaltene linker sites has been extensively discussed in the literature. It was stated: “If the archipelago structures are bridged by cycloalkane rather than linear alkane linkages much of the controversy between the molecular architecture models would be resolved”.¹³ Unfortunately, naphthenes/cycloalkanes cannot be distinguished from the corresponding alkenes via the soft ionization techniques, but the cycloalkanes were detected by GC–EI–QMS only with a minor abundance (in comparison to alkane pyrolytic fragments). Moreover, taking into account the dominance of alkenes, as a product of the thermal cracking of alkylation side chains, the presence of cycloalkane bridging might be a less common structural motive.

According to the mass loss curves discussed above, roughly 40 wt % of the asphaltene sample remains after 600 °C treatment. During pyrolysis, high aromatic island structures can release hydrogen and form a stable coke residue. This carbonization will involve various reactions.⁷⁴ It was shown that aliphatic moieties reveal a higher alteration degree compared to the relatively stable aromatic core.⁷⁵ In this study, the evolved gas is analyzed, and the exact nature of the residue is not a relevant hindering. Furthermore, the reaction parameter, e.g., pressure, reaction time, etc., for which these pathways were shown to be significant, i.e., visbreaking/coking in the refinery, are much harsher than the conditions applied in this study.^{76,77}

Thermal decomposition in thermogravimetry of asphaltenes was reported to be a first-order reaction and relatively quick at temperatures above 440 °C. These complex thermal degradation pathways potentially limit the thermal analysis approach applied upon asphaltenes. Nonetheless, direct infusion APPI FT–MS of the exact same asphaltene within the Asphaltene Characterization Interlaboratory Study for PetroPhase 2017 revealed DBE values of 25–30 for the intact molecules and a loss of DBE during CID, which consolidates the presented interpretation and supports our molecular architecture hypothesis. The findings of thin-film pyrolysis on asphaltenes also suggest bridged structures present in a significant concentration.⁷⁸

Table 1 summarizes the main aspects of the individual techniques and their respective findings. SPI revealed a dominant alkene/alkane pattern, caused by cracking of alkylation sites and verified with Pyr–GC. REMPI exhibits the PAH pattern selectively and even-numbered m/z homologue series as well as tentatively assigned carbazole and acridine derivatives, indicated by even m/z values. Sulfur-containing aromatic structures are detectable, but the short lifetime of their first excited state required for REMPI leads to a very low signal intensity. For polycyclic aromatic sulfur hydrocarbon (PASH) detection, APPI is the method of choice, and the sulfur species could be easily identified, as shown above. APCI is sensitive toward oxygenated compounds, but only a minor proportion of thermally stable oxygen-containing species was observed in the asphaltene pyrolysis effluent. APCI, APPI, and REMPI enable a sensitive

Table 1. Compilation of the Applied Techniques, Their Essential Characteristics, and the Most Significant Results of the Investigation of the PetroPhase 2017 Asphaltene and Parent Crude Oil

method	(1) TD/Pyr-GC-EI-QMS	(2) TG SPI TOF-MS	(3) TG REMPI TOF-MS	(4) TGAPPIFT-ICRMS	(5) TGAPCIFT-ICRMS	
full name	thermal desorption/pyrolysis gas chromatography electron ionization quadrupole mass spectrometry	thermogravimetry single-photon ionization time-of-flight mass spectrometry	thermogravimetry resonance-enhanced multiphoton ionization time-of-flight mass spectrometry	thermogravimetry atmospheric pressure photon ionization Fourier transform ion cyclotron resonance mass spectrometry	thermogravimetry atmospheric pressure chemical ionization Fourier transform ion cyclotron resonance mass spectrometry	
concept	ionization	70 eV electron impact, hard	118 nm single-photon ionization, soft	266 nm resonance-enhanced multiphoton ionization, soft	Kr VUV lamp with 10/10.6 eV (124/117 nm), soft	corona discharge chemical ionization at a 3000 μ A stainless-steel needle, soft
	analyzer	nominal resolution quadrupole with secondary electron multiplier, gas chromatography with separation and retention time information (structure)	reflectron time-of-flight with multichannel plate detection, nominal resolving power, high acquisition rate	reflectron time-of-flight with multichannel plate detection, nominal resolving power, high acquisition rate	ion cyclotron resonance with 7 T magnet (ParaCell, Bruker), ultrahigh resolution (260000 at m/z 400)	ion cyclotron resonance with 7 T magnet (ParaCell, Bruker), ultrahigh resolution (260000 at m/z 400)
detectable compounds	ionization of all organic and inorganic species (universal), gas chromatographic limitation in volatility	species with ionization energy below 10.5 eV, universal for most hydrocarbons	aromatic hydrocarbons with stable intermediate state	semi-polar and nonpolar components, highly efficient for sulfur-containing species	polar and semi-polar constituents, sensitive toward oxygenated species	
what was found?	PetroPhase C ₇ asphaltene	no signal in the thermal desorption (at 300 °C), dominant alkene and alkane pattern, mainly side-chain information, less abundant	intense alkene pattern (C ₃₋₃₅) peaking at propane and an exponential decrease, high abundant H ₂ S	1-5-ring aromatics and their alkylated species up to m/z 500 peaking at m/z 224, 2-3 ring with 3-10 alkylation on average	intense homologue series of benzothiophene with alkane and alkene side chains	intense homologue series of benzothiophene with alkane and alkene side chains, oxygenated species, e.g., CHO and CHSO

detection of aromatic hydrocarbon structures. All three techniques found 2-4-ring PAHs with a DBE of 6-13 as the most abundant constituents of the asphaltene thermal degradation.

CONCLUSION

The thermal analysis of a C₇ asphaltene as well as its parent crude oil and the comprehensive molecular description of the evolved gas mixture were successfully conducted deploying three different couplings and five different ionization techniques. We showed that no significant amount of material evaporates in the desorption phase (<300 °C), whereas in the pyrolysis phase (>~320 °C) a complex variety of thermal decomposition products was detected. A residue of roughly 50 wt % remains after pyrolysis and can be evaporated nearly completely under an oxidative atmosphere at 800-1000 °C. Thus, the asphaltene sample, distributed within the Asphaltene Characterization Interlaboratory Study for PetroPhase 2017, was proven to be carefully prepared and devoid of desorbable co-precipitates.

The combination of different ionization schemes and mass spectrometric analyzers allowed for a more comprehensive chemical description and validation of the pyrolysis effluent. APCI as well as the photoionization techniques allow for a fragment-free characterization, whereas GC-EI partially allows for the validation of structural motives. Side-chain loss dominates the pyrolysis pattern, revealed as alkenes and alkanes via EI and SPI as well as aromatics detected via REMPI, APPI, and APCI. The thermal fragments and field desorption mass spectrometric results were used for an indirect assessment of the molecular architecture. The findings strongly indicate a molecular structure type with several aromatic cores (mainly 2-4-ring systems) linked by aliphatic side chains. Thermal decomposition

of the aromatic core in the proposed island structure type can happen, e.g., along partially saturated ring systems, but is less favorable. Therefore, we suggest archipelago-type asphaltenes be dominant in the PetroPhase 2017 asphaltene. Direct infusion measurements with APPI and CID on an ultrahigh-resolution mass spectrometer on the same sample give evidence for this hypothesis as well.

We have proven that soft ionization is crucial for the specification of the effluent obtained from asphaltene and parent crude oil thermal analysis. Conventional TD/Pyr-GC-EI-QMS delivers valuable information that is, however, not sufficient for the molecular characterization of these ultracomplex sample materials. Investigation of the thermal behavior of standard substances, which mimic each of the suggested architecture types, will be performed in future work, e.g., to address residue and coke formation. Additional information on nitrogen-containing species is obtainable by applying electrospray ionization. Nonetheless, direct infusion experiments most often struggle with the high dynamic range and ultrahigh complexity of these sample materials, and substantial effort has to be taken to generate valuable spectra, e.g., by deploying high-field magnets, acquisition of narrow m/z bands, or chromatographic separation. As for the thermal analysis approaches used in this study, the sample can be used directly without any pretreatment.

The high potential of evolved gas analysis coupled to mass spectrometry and, in particular, the combination of several ionization techniques will stimulate further studies on troublemakers in the petrochemical industry, such as resins, naphthenates, and other deposits, as well as on asphaltenes from a different origin. Additionally, analyzing the residue formed at 600 °C thermal treatment, e.g., via direct infusion or laser desorption high-resolution mass spectrometric techniques, will

increase the understanding of the thermal behavior and allow for further structural assignments.

■ ASSOCIATED CONTENT

Supporting Information

The Supporting Information is available free of charge on the ACS Publications website at DOI: [10.1021/acs.energyfuels.7b02762](https://doi.org/10.1021/acs.energyfuels.7b02762).

Mass loss curves for the investigation of the parent crude oil and asphaltene with the two deployed thermogravimetric systems (Figure S1), chromatograms (TIC and EIC for m/z 55 and 57) and survey view (m/z versus retention time) of the desorption and pyrolysis gas chromatographic measurements (Figures S2–S5), average mass spectra of the crude oil and asphaltene for the photoionization TOF–MS analysis (Figure S6), average CID APCI and APPI mass spectra for the asphaltene pyrolysis (Figure S7), average field desorption mass spectrum (Figure S8), and schematic concept of the thermal decomposition products assembled to the intact molecular weight given by FD–MS (Figure S9) (PDF)

■ AUTHOR INFORMATION

Corresponding Author

*E-mail: christopher.rueger@uni-rostock.de.

ORCID

Christopher P. Rüger: [0000-0001-9634-9239](https://orcid.org/0000-0001-9634-9239)

Ralf Zimmermann: [0000-0002-6280-3218](https://orcid.org/0000-0002-6280-3218)

Notes

The authors declare no competing financial interest.

■ ACKNOWLEDGMENTS

The authors thank the German Research Foundation (DFG) for funding of the Bruker FT-ICR MS (INST 264/56). The authors thank Pierre Giusti for the opportunity to participate in the Asphaltene Characterization Interlaboratory Study for PetroPhase 2017, which is a promising and unique attempt to study the exact same complex sample with various state-of-the-art techniques. The authors thank Prof. Peter Leinweber and Kai-Uwe Eckhardt from the Faculty of Agricultural and Environmental Sciences of the University of Rostock for the supporting FD–MS measurements.

■ REFERENCES

- (1) Fahim, M. A.; Alshahaf, T. A.; Elkilani, A. S. *Fundamentals of Petroleum Refining*, 1st ed.; Elsevier: Amsterdam, Netherlands, 2010.
- (2) Kandiyoti, R. *Solid Fuels and Heavy Hydrocarbon Liquids: Thermal Characterization and Analysis*, 2nd ed.; Elsevier Science: Kent, U.K., 2017.
- (3) Speight, J. G. *The Chemistry and Technology of Petroleum*, 4th ed.; CRC Press (Taylor & Francis Group): Boca Raton, FL, 2007.
- (4) Rodgers, R. P.; Schaub, T. M.; Marshall, A. G. *Petroleomics: MS Returns to Its Roots*. *Anal. Chem.* **2005**, *77* (1), 20 A–27 A.
- (5) Nizio, K. D.; McGinitie, T. M.; Harynuk, J. J. Comprehensive multidimensional separations for the analysis of petroleum. *Journal of chromatography. A* **2012**, *1255*, 12–23.
- (6) *Asphaltenes, Heavy Oils, and Petroleomics*; Mullins, O. C., Sheu, E. Y., Hammami, A., Marshall, A. G., Eds.; Springer: New York, 2007; DOI: [10.1007/0-387-68903-6](https://doi.org/10.1007/0-387-68903-6).
- (7) Mullins, O. C.; Pomerantz, A. E.; Zuo, J. Y.; Dong, C. Downhole fluid analysis and asphaltene science for petroleum reservoir evaluation. *Annu. Rev. Chem. Biomol. Eng.* **2014**, *5*, 325–345.
- (8) Marshall, A. G.; Rodgers, R. P. *Petroleomics: The next grand challenge for chemical analysis*. *Acc. Chem. Res.* **2004**, *37* (1), 53–59.

(9) Marshall, A. G.; Rodgers, R. P. *Petroleomics: Chemistry of the underworld*. *Proc. Natl. Acad. Sci. U. S. A.* **2008**, *105* (47), 18090–18095.

(10) George, G. N.; Gorbaty, M. L. Sulfur K-edge x-ray absorption spectroscopy of petroleum asphaltenes and model compounds. *J. Am. Chem. Soc.* **1989**, *111* (9), 3182–3186.

(11) Mitra-Kirtley, S.; Mullins, O. C.; van Elp, J.; George, S. J.; Chen, J.; Cramer, S. P. Determination of the nitrogen chemical structures in petroleum asphaltenes using XANES spectroscopy. *J. Am. Chem. Soc.* **1993**, *115* (1), 252–258.

(12) Pomerantz, A. E.; Seifert, D. J.; Bake, K. D.; Craddock, P. R.; Mullins, O. C.; Kodalen, B. G.; Mitra-Kirtley, S.; Bolin, T. B. Sulfur Chemistry of Asphaltenes from a Highly Compositionally Graded Oil Column. *Energy Fuels* **2013**, *27* (8), 4604–4608.

(13) Podgorski, D. C.; Corilo, Y. E.; Nyadong, L.; Lobodin, V. V.; Bythell, B. J.; Robbins, W. K.; McKenna, A. M.; Marshall, A. G.; Rodgers, R. P. Heavy Petroleum Composition. 5. Compositional and Structural Continuum of Petroleum Revealed. *Energy Fuels* **2013**, *27* (3), 1268–1276.

(14) Materazzi, S.; Risoluti, R. Evolved Gas Analysis by Mass Spectrometry. *Appl. Spectrosc. Rev.* **2014**, *49* (8), 635–665.

(15) Materazzi, S.; Vecchio, S. Recent Applications of Evolved Gas Analysis by Infrared Spectroscopy (IR-EGA). *Appl. Spectrosc. Rev.* **2013**, *48* (8), 654–689.

(16) Materazzi, S.; Gentili, A.; Curini, R. Applications of evolved gas analysis Part 2: EGA by mass spectrometry. *Talanta* **2006**, *69* (4), 781–794.

(17) Rustschev, D. D. Application of thermal analysis for investigating liquid fuels, petroleum- and coke-chemical products. *Thermochim. Acta* **1990**, *168*, 261–271.

(18) Materazzi, S.; Vecchio, S. Evolved Gas Analysis by Mass Spectrometry. *Appl. Spectrosc. Rev.* **2011**, *46* (4), 261–340.

(19) Holdiness, M. R. Evolved gas analysis by mass spectrometry: A review. *Thermochim. Acta* **1984**, *75* (3), 361–399.

(20) Huang, J. Thermal Degradation of Asphaltene and Infrared Characterization of Its Degraded Fractions. *Pet. Sci. Technol.* **2006**, *24* (9), 1089–1095.

(21) Alosmanov, R.; Wolski, K.; Matuschek, G.; Magerramov, A.; Azizov, A.; Zimmermann, R.; Aliyev, E.; Zapotoczny, S. Effect of functional groups on the thermal degradation of phosphorus- and phosphorus/nitrogen-containing functional polymers. *J. Therm. Anal. Calorim.* **2017**, *109*, 130–139.

(22) Streibel, T.; Geißler, R.; Saraji-Bozorgzad, M.; Sklorz, M.; Kaisersberger, E.; Denner, T.; Zimmermann, R. Evolved gas analysis (EGA) in TG and DSC with single photon ionisation mass spectrometry (SPI-MS): Molecular organic signatures from pyrolysis of soft and hard wood, coal, crude oil and ABS polymer. *J. Therm. Anal. Calorim.* **2009**, *96* (3), 795–804.

(23) Geissler, R.; Saraji-Bozorgzad, M. R.; Gröger, T.; Fendt, A.; Streibel, T.; Sklorz, M.; Krooss, B. M.; Fuhrer, K.; Gonin, M.; Kaisersberger, E.; Denner, T.; Zimmermann, R. Single Photon Ionization Orthogonal Acceleration Time-of-Flight Mass Spectrometry and Resonance Enhanced Multiphoton Ionization Time-of-Flight Mass Spectrometry for Evolved Gas Analysis in Thermogravimetry: Comparative Analysis of Crude Oils. *Anal. Chem.* **2009**, *81* (15), 6038–6048.

(24) Wohlfahrt, S.; Fischer, M.; Saraji-Bozorgzad, M.; Matuschek, G.; Streibel, T.; Post, E.; Denner, T.; Zimmermann, R. Rapid comprehensive characterization of crude oils by thermogravimetry coupled to fast modulated gas chromatography-single photon ionization time-of-flight mass spectrometry. *Anal. Bioanal. Chem.* **2013**, *405* (22), 7107–7116.

(25) Béhar, F.; Pelet, R. Pyrolysis-gas chromatography applied to organic geochemistry. *J. Anal. Appl. Pyrolysis* **1985**, *8*, 173–187.

(26) Garg, A. K.; Philp, R. P. Pyrolysis-gas chromatography of asphaltenes/kerogens from source rocks of the Gandhar Field, Cambay Basin, India. *Org. Geochem.* **1994**, *21* (3–4), 383–392.

- (27) Mascherpa, A.; Casalini, A. Pyrolysis GC-MS of asphaltenes from straight-run and visbreaker bitumens. *J. High Resolut. Chromatogr.* **1988**, *11* (3), 296–299.
- (28) Nali, M.; Corana, F.; Montanari, L. Pyrolysis/gas chromatography/mass spectrometry in the analysis of asphaltenes. *Rapid Commun. Mass Spectrom.* **1993**, *7* (7), 684–687.
- (29) Sarmah, M. K.; Borthakur, A.; Dutta, A. Pyrolysis of petroleum asphaltenes from different geological origins and use of methyl-naphthalenes and methylphenanthrenes as maturity indicators for asphaltenes. *Bull. Mater. Sci.* **2010**, *33* (4), 509–515.
- (30) Solli, H.; Leplat, P. Pyrolysis-gas chromatography of asphaltenes and kerogens from source rocks and coals—A comparative structural study. *Org. Geochem.* **1986**, *10* (1–3), 313–329.
- (31) Speight, J. G.; Pancirov, R. J. Structural types in petroleum asphaltenes as deduced from pyrolysis/gas chromatography/mass spectrometry. *Liq. Fuels Technol.* **1984**, *2* (3), 287–305.
- (32) Li, D.-X.; Gan, L.; Bronja, A.; Schmitz, O. J. Gas chromatography coupled to atmospheric pressure ionization mass spectrometry (GC-API-MS): Review. *Anal. Chim. Acta* **2015**, *891*, 43–61.
- (33) Kök, M. V. Thermal analysis applications in fossil fuel science: Literature survey. *J. Therm Anal Calorim* **2002**, *68* (3), 1061–1077.
- (34) Fendt, A.; Geissler, R.; Streibel, T.; Sklorz, M.; Zimmermann, R. Hyphenation of two simultaneously employed soft photo ionization mass spectrometers with thermal analysis of biomass and biochar. *Thermochim. Acta* **2013**, *551*, 155–163.
- (35) Fischer, M.; Wohlfahrt, S.; Saraji-Bozorgzad, M.; Matuschek, G.; Post, E.; Denner, T.; Streibel, T.; Zimmermann, R. Thermal analysis/evolved gas analysis using single photon ionization. *J. Therm. Anal. Calorim.* **2013**, *113* (3), 1667–1673.
- (36) Hölzer, J.; Fischer, M.; Gröger, T.; Streibel, T.; Saraji-Bozorgzad, M.; Wohlfahrt, S.; Matuschek, G.; Zimmermann, R. Hyphenation of thermogravimetry and soft single photon ionization-ion trap mass spectrometry (TG-SPI-ITMS) for evolved gas analysis. *J. Therm. Anal. Calorim.* **2014**, *116* (3), 1471–1479.
- (37) Streibel, T.; Fendt, A.; Geißler, R.; Kaisersberger, E.; Denner, T.; Zimmermann, R. Thermal analysis/mass spectrometry using soft photo-ionisation for the investigation of biomass and mineral oils. *J. Therm. Anal. Calorim.* **2009**, *97* (2), 615–619.
- (38) Dyszel, S. M. Thermogravimetry coupled with atmospheric pressure ionization mass spectrometry. A new combined technique. *Thermochim. Acta* **1983**, *61* (1–2), 169–183.
- (39) Dyszel, S. M. Characterization of green coffee beans by combined thermogravimetric analysis/atmospheric pressure chemical ionization mass spectrometry. *Thermochim. Acta* **1985**, *87*, 89–98.
- (40) Prime, R. B.; Shushan, B. Thermogravimetric analyzer/atmospheric pressure chemical ionization tandem triple quadrupole mass spectrometer system for evolved gas analysis. *Anal. Chem.* **1989**, *61* (11), 1195–1201.
- (41) Rüger, C. P.; Miersch, T.; Schwemer, T.; Sklorz, M.; Zimmermann, R. Hyphenation of Thermal Analysis to Ultrahigh-Resolution Mass Spectrometry (Fourier Transform Ion Cyclotron Resonance Mass Spectrometry) Using Atmospheric Pressure Chemical Ionization For Studying Composition and Thermal Degradation of Complex Materials. *Anal. Chem.* **2015**, *87* (13), 6493–6499.
- (42) Streibel, T.; Zimmermann, R. Resonance-enhanced multiphoton ionization mass spectrometry (REMPI-MS): Applications for process analysis. *Annu. Rev. Anal. Chem.* **2014**, *7*, 361–381.
- (43) Zimmermann, R. Photo ionisation in mass spectrometry: Light, selectivity and molecular ions. *Anal. Bioanal. Chem.* **2013**, *405* (22), 6901–6905.
- (44) Himmelsbach, M.; Buchberger, W.; Reingruber, E. Determination of polymer additives by liquid chromatography coupled with mass spectrometry. A comparison of atmospheric pressure photoionization (APPI), atmospheric pressure chemical ionization (APCI), and electrospray ionization (ESI). *Polym. Degrad. Stab.* **2009**, *94* (8), 1213–1219.
- (45) Gaspar, A.; Zeller, E.; Lababidi, S.; Reece, J.; Schrader, W. Impact of different ionization methods on the molecular assignments of asphaltenes by FT-ICR mass spectrometry. *Anal. Chem.* **2012**, *84* (12), 5257–5267.
- (46) Farenc, M.; Corilo, Y. E.; Lalli, P. M.; Riches, E.; Rodgers, R. P.; Afonso, C.; Giusti, P. Comparison of Atmospheric Pressure Ionization for the Analysis of Heavy Petroleum Fractions with Ion Mobility-Mass Spectrometry. *Energy Fuels* **2016**, *30* (11), 8896–8903.
- (47) Cai, S.-S.; Syage, J. A. Comparison of atmospheric pressure photoionization, atmospheric pressure chemical ionization, and electrospray ionization mass spectrometry for analysis of lipids. *Anal. Chem.* **2006**, *78* (4), 1191–1199.
- (48) Fischer, M.; Wohlfahrt, S.; Varga, J.; Matuschek, G.; Saraji-Bozorgzad, M. R.; Walte, A.; Denner, T.; Zimmermann, R. Evolution of Volatile Flavor Compounds During Roasting of Nut Seeds by Thermogravimetry Coupled to Fast-Cycling Optical Heating Gas Chromatography-Mass Spectrometry with Electron and Photoionization. *Food Anal. Methods* **2017**, *10* (1), 49–62.
- (49) Fischer, M.; Wohlfahrt, S.; Varga, J.; Saraji-Bozorgzad, M.; Matuschek, G.; Denner, T.; Zimmermann, R. Evolved gas analysis by single photon ionization-mass spectrometry. *J. Therm. Anal. Calorim.* **2014**, *116* (3), 1461–1469.
- (50) Varga, J.; Wohlfahrt, S.; Fischer, M.; Saraji-Bozorgzad, M. R.; Matuschek, G.; Denner, T.; Reller, A.; Zimmermann, R. An evolved gas analysis method for the characterization of sulfur vapor. *J. Therm. Anal. Calorim.* **2017**, *127* (1), 955–960.
- (51) Otto, S.; Erdmann, S.; Streibel, T.; Herlemann, D. P. R.; Schulz-Bull, D.; Zimmermann, R. Pyrolysis-gas chromatography-mass spectrometry with electron-ionization and resonance-enhanced-multiphoton-ionization for the characterization of terrestrial dissolved organic matter in the Baltic Sea. *Anal. Methods* **2016**, *8* (12), 2592–2603.
- (52) Chacón-Patiño, M. L.; Vesga-Martínez, S. J.; Blanco-Tirado, C.; Orrego-Ruiz, J. A.; Gómez-Escudero, A.; Combariza, M. Y. Exploring Occluded Compounds and Their Interactions with Asphaltene Networks Using High-Resolution Mass Spectrometry. *Energy Fuels* **2016**, *30* (6), 4550–4561.
- (53) Otto, S.; Streibel, T.; Erdmann, S.; Sklorz, M.; Schulz-Bull, D.; Zimmermann, R. Application of pyrolysis-mass spectrometry and pyrolysis-gas chromatography-mass spectrometry with electron-ionization or resonance-enhanced-multi-photon ionization for characterization of crude oils. *Anal. Chim. Acta* **2015**, *855*, 60–69.
- (54) Otto, S.; Streibel, T.; Erdmann, S.; Klingbeil, S.; Schulz-Bull, D.; Zimmermann, R. Pyrolysis-gas chromatography-mass spectrometry with electron-ionization or resonance-enhanced-multi-photon-ionization for characterization of polycyclic aromatic hydrocarbons in the Baltic Sea. *Mar. Pollut. Bull.* **2015**, *99* (1–2), 35–42.
- (55) Streibel, T.; Mitschke, S.; Adam, T.; Weh, J.; Zimmermann, R. Thermal desorption/pyrolysis coupled with photo ionisation time-of-flight mass spectrometry for the analysis and discrimination of pure tobacco samples. *J. Anal. Appl. Pyrolysis* **2007**, *79* (1–2), 24–32.
- (56) Zimmermann, R.; Saraji-Bozorgzad, M.; Grimmer, C.; Ulbrich, A.; Streibel, T. Erdöl in seine Bestandteile zerlegen und charakterisieren. *Nachr. Chem.* **2016**, *64* (7–8), 751–754.
- (57) Mühlberger, F.; Hafner, K.; Kaesdorf, S.; Ferge, T.; Zimmermann, R. Comprehensive on-line characterization of complex gas mixtures by quasi-simultaneous resonance-enhanced multiphoton ionization, vacuum-UV single-photon ionization, and electron impact ionization in a time-of-flight mass spectrometer: Setup and instrument characterization. *Anal. Chem.* **2004**, *76* (22), 6753–6764.
- (58) Schiewek, R.; Lorenz, M.; Giese, R.; Brockmann, K.; Benter, T.; Gäb, S.; Schmitz, O. J. Development of a multipurpose ion source for LC-MS and GC-API MS. *Anal. Bioanal. Chem.* **2008**, *392* (1–2), 87–96.
- (59) Calemma, V.; Rausa, R. Thermal decomposition behaviour and structural characteristics of asphaltenes. *J. Anal. Appl. Pyrolysis* **1997**, *40–41*, 569–584.
- (60) Gonçalves, M. L. A.; Teixeira, M. A. G.; Pereira, R. C. L.; Mercury, R. L. P.; Matos, J. R. Contribution of thermal analysis for characterization of asphaltenes from Brazilian crude oil. *J. Therm Anal Calorim* **2001**, *64* (2), 697–706.

- (61) Nali, M.; Calemma, V.; Montanari, L. Pyrolysis/gas chromatography/mass spectrometry of asphaltene fractions. *Org. Mass Spectrom.* **1994**, *29* (11), 607–614.
- (62) Hanley, L.; Zimmermann, R. Light and molecular ions: The emergence of vacuum UV single-photon ionization in MS. *Anal. Chem.* **2009**, *81* (11), 4174–4182.
- (63) Islas, C. A.; Suelves, I.; Carter, J. F.; Herod, A. A.; Kandiyoti, R. Pyrolysis-gas chromatography/mass spectrometry of a coal extract and its fractions separated by planar chromatography: Correlation of structural features with molecular mass. *Rapid Commun. Mass Spectrom.* **2000**, *14* (19), 1766–1782.
- (64) Eschner, M. S.; Zimmermann, R. Determination of photoionization cross-sections of different organic molecules using gas chromatography coupled to single-photon ionization (SPI) time-of-flight mass spectrometry (TOF-MS) with an electron-beam-pumped rare gas excimer light source (EBEL): Influence of molecular structure and analytical implications. *Appl. Spectrosc.* **2011**, *65* (7), 806–816.
- (65) Boesl, U.; Neusser, H. J.; Schlag, E. W. Multi-photon ionization in the mass spectrometry of polyatomic molecules: Cross sections. *Chem. Phys.* **1981**, *55* (2), 193–204.
- (66) Adam, T. W.; Clairotte, M.; Streibel, T.; Elsasser, M.; Pommeres, A.; Manfredi, U.; Carriero, M.; Martini, G.; Sklorz, M.; Krasenbrink, A.; Astorga, C.; Zimmermann, R. Real-time analysis of aromatics in combustion engine exhaust by resonance-enhanced multiphoton ionisation time-of-flight mass spectrometry (REMPI-TOF-MS): A robust tool for chassis dynamometer testing. *Anal. Bioanal. Chem.* **2012**, *404* (1), 273–276.
- (67) Pereira, T. M. C.; Vanini, G.; Tose, L. V.; Cardoso, F. M. R.; Fleming, F. P.; Rosa, P. T. V.; Thompson, C. J.; Castro, E. V. R.; Vaz, B. G.; Romão, W. FT-ICR MS analysis of asphaltene: Asphaltenes go in, fullerenes come out. *Fuel* **2014**, *131*, 49–58.
- (68) Korsten, H. Characterization of hydrocarbon systems by DBE concept. *AIChE J.* **1997**, *43* (6), 1559–1568.
- (69) Cho, Y.; Kim, Y. H.; Kim, S. Planar limit-assisted structural interpretation of saturates/aromatics/resins/asphaltenes fractionated crude oil compounds observed by Fourier transform ion cyclotron resonance mass spectrometry. *Anal. Chem.* **2011**, *83* (15), 6068–6073.
- (70) Rüger, C. P.; Sklorz, M.; Schwemer, T.; Zimmermann, R. Characterisation of ship diesel primary particulate matter at the molecular level by means of ultra-high-resolution mass spectrometry coupled to laser desorption ionisation-comparison of feed fuel, filter extracts and direct particle measurements. *Anal. Bioanal. Chem.* **2015**, *407* (20), 5923–5937.
- (71) Badre, S.; Carla Goncalves, C.; Norinaga, K.; Gustavson, G.; Mullins, O. C. Molecular size and weight of asphaltene and asphaltene solubility fractions from coals, crude oils and bitumen. *Fuel* **2006**, *85* (1), 1–11.
- (72) Groenzin, H.; Mullins, O. C. Asphaltene Molecular Size and Structure. *J. Phys. Chem. A* **1999**, *103* (50), 11237–11245.
- (73) Groenzin, H.; Mullins, O. C. Molecular Size and Structure of Asphaltenes from Various Sources. *Energy Fuels* **2000**, *14* (3), 677–684.
- (74) Zhao, Y.; Wei, F.; Yu, Y. Effects of reaction time and temperature on carbonization in asphaltene pyrolysis. *J. Pet. Sci. Eng.* **2010**, *74* (1–2), 20–25.
- (75) Douda, J.; Alvarez, R.; Navarrete Bolaños, J. Characterization of Maya Asphaltene and Maltene by Means of Pyrolysis Application. *Energy Fuels* **2008**, *22* (4), 2619–2628.
- (76) Alshareef, A. H.; Scherer, A.; Tan, X.; Azyat, K.; Stryker, J. M.; Tykwinski, R. R.; Gray, M. R. Formation of Archipelago Structures during Thermal Cracking Implicates a Chemical Mechanism for the Formation of Petroleum Asphaltenes. *Energy Fuels* **2011**, *25* (5), 2130–2136.
- (77) Yasar, M.; Trauth, D. M.; Klein, M. T. Asphaltene and Resid Pyrolysis. 2. The Effect of Reaction Environment on Pathways and Selectivities. *Energy Fuels* **2001**, *15* (3), 504–509.
- (78) Karimi, A.; Qian, K.; Olmstead, W. N.; Freund, H.; Yung, C.; Gray, M. R. Quantitative Evidence for Bridged Structures in Asphaltenes by Thin Film Pyrolysis. *Energy Fuels* **2011**, *25* (8), 3581–3589.